Structural Chemistry (2021) 32:1553–1562
https://doi.org/10.1007/s11224-021-01768-0

ORIGINAL RESEARCH

Synthesis and crystal structures of 7,8-bromo (dibromo) -3-*tert*-butylpyrazolo[5,1-*c*][1,2,4]triazines

Sergey M. Ivanov[1] · Denis S. Koltun[1]

Received: 1 March 2021 / Accepted: 15 March 2021 / Published online: 29 March 2021

Abstract

Single crystal structures in a series of 7-bromo-, 8-bromo-, and 7,8-dibromo-3-*tert*-butylpyrazolo[5,1-*c*][1,2,4]triazin-4(1*H*)-ones have been investigated by X-ray diffraction. Novel 7-bromo- and 7,8-dibromo-3-*tert*-butylpyrazolo[5,1-*c*][1,2,4]triazines were synthesized by reduction of triazine carbonyl with dehydrative aromatization in acidic media, and their XRD structural features were compared with that of the 4-oxo analogs. The lengths and bond angles and the packing of molecules in crystals have been considered. Non-valence interactions for some of the studied compounds were observed. Correlations between the presence of bromine atoms at different positions and structural features are determined.

Keywords Crystal structure, X-ray diffraction, 1,2,4-Triazine, Pyrazolo[5,1-*c*][1,2,4]triazine

Introduction

The qualitative and quantitative structural aspects of heterocyclic compounds are of interest in terms of their utility for the certain mechanistic and synthetic studies [1–3], as well as for various biological applications [4–6]. It is known that most of the six-membered saturated heterocycles prefer the chair conformations [7, 8], while the aromatics are nearly planar. The significant deviations can often be the result of combination of steric and electronic factors [9].

Fused triazines exhibit diverse conformational behavior depending on the nature of an annulated ring [10, 11]. Azolo[1,2,4] triazines [12] constitute an important class of such compounds which have found broad use as effective antiviral agents, e.g., 1,2,4-triazolo[5,1-*c*][1,2,4]triazine (triazavirin) [13] and pyrrolo[2,1-*f*][1,2,4]triazine (remdesivir) [14, 15]. Nevertheless, the structural features of such systems are still relatively poorly studied. In continuation of our studies on the chemical and structural properties of functionalized pyrazolo[5,1-*c*][1,2,4]triazines [16–21], in the present work, we discuss the single crystal structures in a series of brominated 4-oxo- and novel 4-unsubstituted-3-*tert*-butylpyrazolo[5,1-*c*][1,2,4]triazines, including bond lengths and angles, non-valence interactions, and packing modes.

✉ Sergey M. Ivanov
sergey13iv1@mail.ru

[1] Zelinsky Institute of Organic Chemistry, Russian Academy of Sciences, 47 Leninsky Prospect, Moscow, Russian Federation

Experimental

General experimental remarks

Melting points were determined on a STUART Melting point SMP30 apparatus. IR spectra were recorded in KBr pellets using Agilent Cary 660 FTIR infrared spectrophotometer. NMR spectra were recorded on Bruker AM-300 or AV-600 spectrometers operating at working frequencies of 300 (^{1}H), 75 or 151 MHz (^{13}C). Chemical shifts were related to that of the $CHCl_3$ (^{1}H), or $CDCl_3$ (^{13}C). High resolution mass spectra were recorded on a Bruker MicroTOF II instrument in positive ion mode (capillary voltage 4500 V) using electrospray ionization (ESI) and methanol or acetonitrile as a solvent. Elemental analysis was performed on a PerkinElmer Series II 2400 Elemental Analyzer. All reagents were obtained from commercial sources and used without additional purification. Starting compounds **1a**,**b**, **2a-d**, and **3a** were synthesized as described in literature (Scheme 1) [17–20].

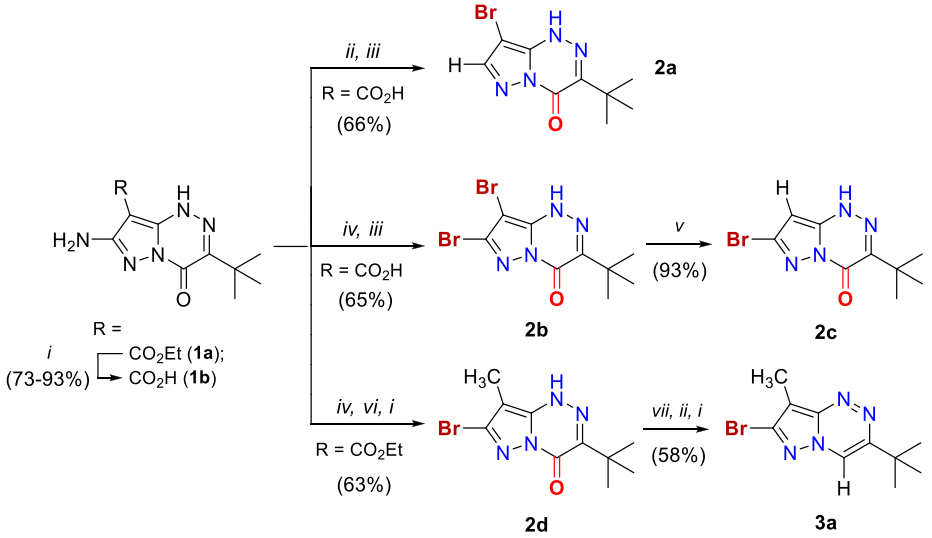

Reagents and conditions:

i: KOH or K_2CO_3, EtOH/H_2O, $NBu_4^+Br^-$ (cat.), 20–100°C, then HCl/H_2O, 0 °C (for **1b** only);

ii: MeOH or *i*-PrOH or neat (for **3a** only), *t*-BuONO, Δ 5-15 min;

iii: NBS, Et_3N, EtOAc or MeCN, 0–25 °C, 5 min – 1 h;

iv: TMSBr/*t*-BuONO, MeCN, Δ 15 min;

v: NaH, THF, 20°C, 15 min, then *n*-BuLi, THF, –97 °C, 3 min, then KH_2PO_4, H_2O, 0 °C;

vi: B_2H_6, Et_2O/THF, 10–20 °C, 7 h;

vii: BH_3/BF_3, Et_2O/THF, 0–20 °C, 2 weeks.

Scheme 1

General procedure for the synthesis of compounds 3b and 3c (Scheme 2)

Compound **1b** (1.23 g, 4.90 mmol) was dissolved in a mixture of DMF (10 ml), NEt_3 (1 ml, 7.17 mmol), and Boc_2O (1.1 g, 5.04 mmol). To the resulting solution, NaN_3 (10 mg, 1.53 × 10^{-4} mol) was added, and the reaction mixture was heated at 60 °C for 15 min with stirring. Then, it was cooled and added to 100 ml of water. The formed precipitate was filtered, washed with H_2O (3 × 50 ml) and heptane (2 × 15 ml), dried

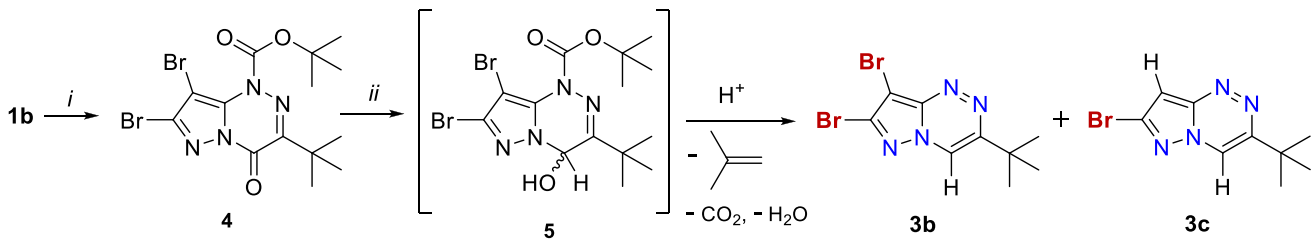

Reagents and conditions:

i: Boc_2O, NaN_3, $NBu_4^+Br^-$ (cat.), dioxane or DMF, 40–80 °C, 20–40 min, then TMSBr, *t*-BuONO, MeCN, 0–50 °C, 1.5 h (68%); *ii*: $NaBH_4$, MeOH, r.t. – 50 °C, 1 h, then HCl/H_2O, 0 °C – r.t., 2 h, then Na_2HPO_4, H_2O, r.t., 20 min (15–42% from **1b**).

Scheme 2

Table 1 Crystal data, data collection, and structure refinement for compounds **2a-d**

Compound	2a	2b	2c	2d·DMSO	2d
Formula	$C_9H_{11}BrN_4O$	$C_9H_{10}Br_2N_4O$	$C_9H_{11}BrN_4O$	$C_{12}H_{19}BrN_4O_2S$	$C_{10}H_{13}BrN_4O$
M_r	271.13	350.03	271.13	363.28	285.15
Crystal system	Monoclinic	Orthorhombic	Triclinic	Triclinic	Orthorhombic
Space group	$P2_1/c$	*Pbca*	$P\bar{1}$	$P\bar{1}$	*Pbca*
Unit cell dimensions					
a (Å)	13.0854(3)	11.6162(3)	9.9149(5)	6.9289(2)	11.6416(2)
b (Å)	7.4580(2)	12.1198(3)	11.5754(6)	10.2508(3	12.0120(2)
c (Å)	11.7128(3)	17.1209(4)	12.1650(6)	11.7436(3)	17.1704(3)
β (°)	101.8950(10)	90	67.8606(18)	83.8248(8)	90
Volume, Å^3	1118.52(5)	2410.38(10)	1101.58(10)	793.54(4)	2401.09(7)
Z	4	8	4	2	8
Calcd. density (g/cm^3)	1.610	1.929	1.635	1.520	1.578
μ (mm^{-1})	3.655	6.710	3.711	2.728	3.410
F(000)	544	1360	544	372	1152
Crystal size (mm)	0.57 × 0.15 x 0.09	0.58 × 0.06 × 0.05	0.53 × 0.17 × 0.06	0.59 × 0.54 × 0.48	0.20 × 0.105 × 0.075
Θ range (°)	3.161 to 35.000	2.379 to 39.394	1.951 to 31.000	2.076 to 37.038	2.372 to 34.343
Completeness to Θ_{max}	1.000	0.998	0.999	0.998	0.999
Index ranges	$-21 \le h \le 21$	$-20 \le h \le 20$	$-12 \le h \le 14$	$-11 \le h \le 11$	$-18 \le h \le 18$
	$-12 \le k \le 12$	$-21 \le k \le 21$	$-14 \le k \le 16$ $0 \le l \le 17$	$-17 \le k \le 17$	$-19 \le k \le 19$
	$-18 \le l \le 18$	$-30 \le l \le 30$		$-19 \le l \le 19$	$-27 \le l \le 27$
Reflections					
Measured	36447	117001	7017	50659	64380
Independent [R_{int}]	4906 [0.0427]	7174 [0.0401]	7017 [-]	8101 [0.0345]	5028 [0.0647]
Observed [$I > 2\sigma(I)$]	4010	5697	5650	7446	3567
Parameters, restraints	143, 0	152, 0	284, 2	192, 0	205, 24
R1, wR2 [$I > 2\sigma(I)$]	0.0291, 0.0609	0.0387, 0.0973	0.0773, 0.2019	0.0234, 0.0598	0.0375, 0.0767
R1, wR2 (all data)	0.0429, 0.0661	0.0529, 0.1047	0.0973, 0.2182	0.0269, 0.0614	0.0661, 0.0885
GooF on F^2	1.041	1.117	1.081	1.034	1.043
$\Delta\rho_{max}$, $\Delta\rho_{min}$ (e Å^{-3})	0.621, −0.653	2.112, −0.761	3.108, −1.591	0.462, -0.825	0.465, −0.672
CCDC number	2065233	2065234	2065235	2065237	2065236

Table 2 Crystal data, data collection, and structure refinement for compounds **3a-c**

Compound	3a	3b	3c
Formula	$C_{10}H_{13}BrN_4$	$C_9H_{10}Br_2N_4$	$C_9H_{11}BrN_4$
M_r	269.15	334.03	255.13
Crystal system	Orthorhombic	Monoclinic	Monoclinic
Space group	*Pnma*	$P2_1/n$	$P2_1/n$
Unit cell dimensions			
a (Å)	17.6328(6)	6.8857(4)	6.05670(10)
b (Å)	6.7165(2)	7.3453(4)	12.7391(3)
c (Å)	19.8019(7)	22.5552(14)	13.6146(3)
β (°)	90	90.135(3)	101.5990(10)
Volume, Å^3	2345.15(13)	1140.78(12)	1029.01(4)
Z	8	4	4
Calcd. density (g/cm^3)	1.525	1.945	1.647
μ (mm^{-1})	3.480	7.079	3.961
F(000)	1088	648	512
Crystal ≤ size (mm)	0.57 × 0.38 × 0.23	0.361 × 0.323 × 0.072	0.59 × 0.19 × 0.18
Θ range (°)	2.310 to 33.176	2.917 to 30.998	3.055 to 33.170
Completeness to Θ_{max}	0.999	0.997	1.000
Index ranges	$-27 \le h \le 27$	$-9 \le h \le 9$	$-9 \le h \le 9$
	$-10 \le k \le 10$	$-10 \le k \le 10$	$-19 \le k \le 19$
	$-30 \le l \le 30$	$-32 \le l \le 32$	$-20 \le l \le 20$
Reflections			
Measured	58659	56077	32573
Independent [R_{int}]	4796 [0.0404]	3639 [0.0550]	3935 [0.0328]
Observed [$I > 2\sigma(I)$]	3960	3639	3935
Parameters, restraints	238, 0	139, 0	130, 0
R1, wR2 [$I > 2\sigma(I)$]	0.0283, 0.0691	0.0679, 0.1724	0.0218, 0.0534
R1, wR2 (all data)	0.0388, 0.0747	0.0749, 0.1771	0.0270, 0.0555
GooF on F^2	1.026	1.202	1.045
$\Delta\rho_{max}$, $\Delta\rho_{min}$ (e Å^{-3})	0.480, −0.349	1.807, −1.483	0.415, −0.632
CCDC number	2065238	2065239	2065240

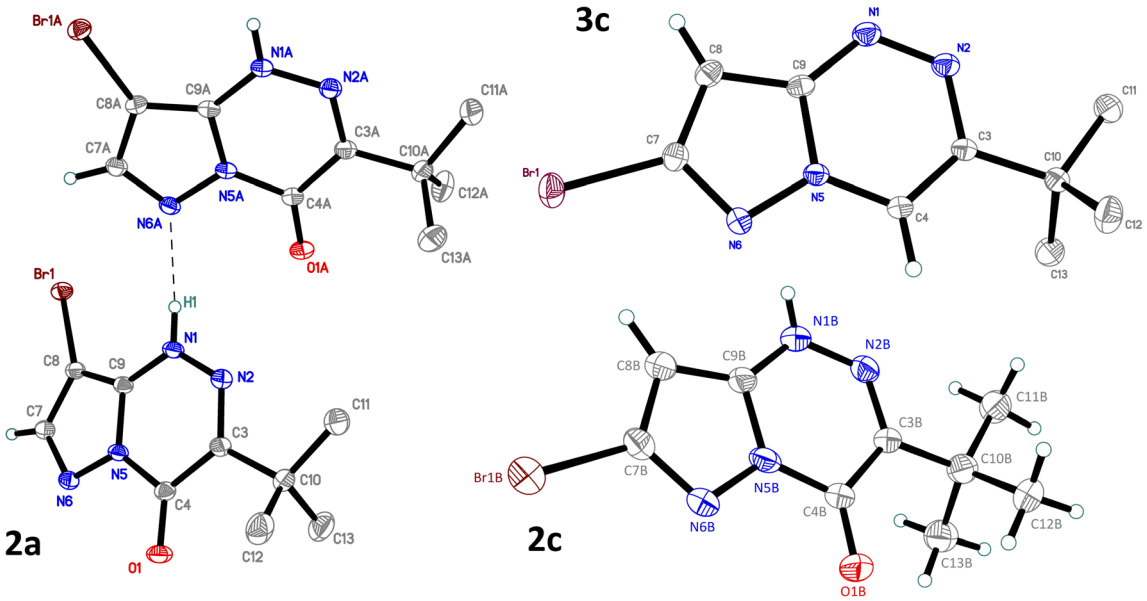

Fig. 1 Molecular structures of **2a**, **2c** and **3c**. H-atoms of methyl groups for **2a** and **3c** are omitted; displacement ellipsoids are shown at the 50% probability level

in air, and suspended in a mixture of TMSBr (4 ml, 30.31 mmol) and MeCN (10 ml). To this suspension, *t*-BuONO (5 ml, 42.04 mmol) was added dropwise over 20 min and with vigorous stirring. After the addition was complete, the black reaction mixture was further stirred for 1 h at 50 °C. After cooling to r.t., MeOH (15 ml) and $NaBH_4$ (1 g, 26.43 mmol) were simultaneously added in small portions with stirring over 30 min. After the addition was complete, the mixture was further stirred at 50 °C for 30 min. Then, it was cooled to 0 °C, conc. HCl/H_2O solution (15 ml) was added slowly, and the red reaction mixture was stirred for 2 h at r.t. Next, H_2O (100 ml), $Na_2HPO_4{\cdot}2H_2O$ (20 g, 112.37 mmol), EtOAc (30 ml), and heptane (50 ml) were added in one portion, and the biphasic mixture was stirred vigorously for 20 min at r.t. The organic phase was separated, dried with crystalline K_2CO_3 and anhydrous $MgSO_4$, and filtered. The solvents were removed in vacuo, and the residue was purified by two-fold flash column chromatography (eluted with EtOAc:heptane = 1:100 – 3:200) to give compounds **3b** and **3c**.

7,8-Dibromo-3-*tert*-butylpyrazolo[5,1-*c*][1,2,4]triazine (3b)

Yellow crystals, yield 0.68 g (2.04 mmol, 42%), mp. 124–125 °C. IR (KBr) ν = 3098, 3068, 2959, 2973, 2931, 2904, 2867 (CH), 1614, 1579, 1512, 1468, 1413, 1364, 1336, 1311, 1282, 1249, 1227, 1199, 1165, 1075, 1025, 934, 950, 874, 765, 729, 645 cm^{-1}. ^1H NMR: (300 MHz, $CDCl_3$) δ 8.31 (s, 1H, C(4)H), 1.55 (s, 9H, C (CH_3)$_3$). $^{13}C\{^1H\}$ NMR: (151 MHz, $CDCl_3$) δ 154.61, 145.92, 136.54 (C(3), C(7), C(8a)), 116.45 (C(4)H), 89.25 (C(8)), 35.04 (C(CH_3)$_3$), 29.10 (C(CH_3)$_3$). HRMS *m/z* ($I_{rel.}$ %) calculated: 334.9325 $[M+H]^+$, found: 334.9332 $[M+H]^+$ (100). Anal. calcd. for $C_9H_{10}Br_2N_4$ (%): C, 32.36, H, 3.02, N, 16.77. Found (%): C, 32.40, H, 3.05, N, 16.72.

7-Bromo-3-*tert*-butylpyrazolo[5,1-*c*][1,2,4]triazine (3c)

Yellow crystals, yield 0.19 g (0.74 mmol, 15%), mp. 112–113 °C. IR (KBr) ν = 3137, 3067, 3015, 2974, 2961, 2930, 2900, 2867 (CH), 1832, 1566, 1579, 1546, 1501, 1462, 1416, 1369, 1312, 1334, 1283,1230, 1249, 1196, 1144, 1117, 1073, 1027, 966, 928, 853, 821, 796, 753, 723, 663, 628, 554, 510, 439 cm^{-1}. ^1H NMR: (300 MHz, $CDCl_3$) δ 8.34 (s, 1H, C(4)H), 7.23 (s, 1H, C(8)H), 1.55 (s, 9H, C(CH_3)$_3$). $^{13}C\{^1H\}$ NMR: (75 MHz, $CDCl_3$, 298 K) δ 154.33, 149.66, 135.41 (C(3), C(7), C(8a)), 116.72 (C(4)H), 100.80 (C(8)H), 35.48 (C(CH_3)$_3$), 29.73 (C(CH_3)$_3$). HRMS *m/z* ($I_{rel.}$ %) calculated: 255.0240 $[M+H]^+$, found: 255.0245 $[M+H]^+$ (100). Anal. calcd. for $C_9H_{11}BrN_4$ (%): C, 42.37, H, 4.35, N, 21.96. Found (%): C, 42.33, H, 4.38, N, 21.94.

For X-ray single crystal studies, all compounds were recrystallized by slow solvent evaporation at r.t. from nearly saturated solutions in ethyl acetate/dimethylsulfoxide mixture (10:1 *v/v*). Crystallization of **2d** from the same solvent mixture provided a mixture of two polymorph modifications: **2d•DMSO** (major component, colorless blocks on a flask's bottom, over 95%) and non-solvated **2d** (minor, colorless blocks on flask's walls).

Fig. 2 Molecular structures of **2d**, **2d·DMSO**, and **3a**, and packing of ▶ compound **3a** in a single crystal. H-atoms of methyl groups for **2d** and **3a** are omitted; displacement ellipsoids are shown at the 50% probability level

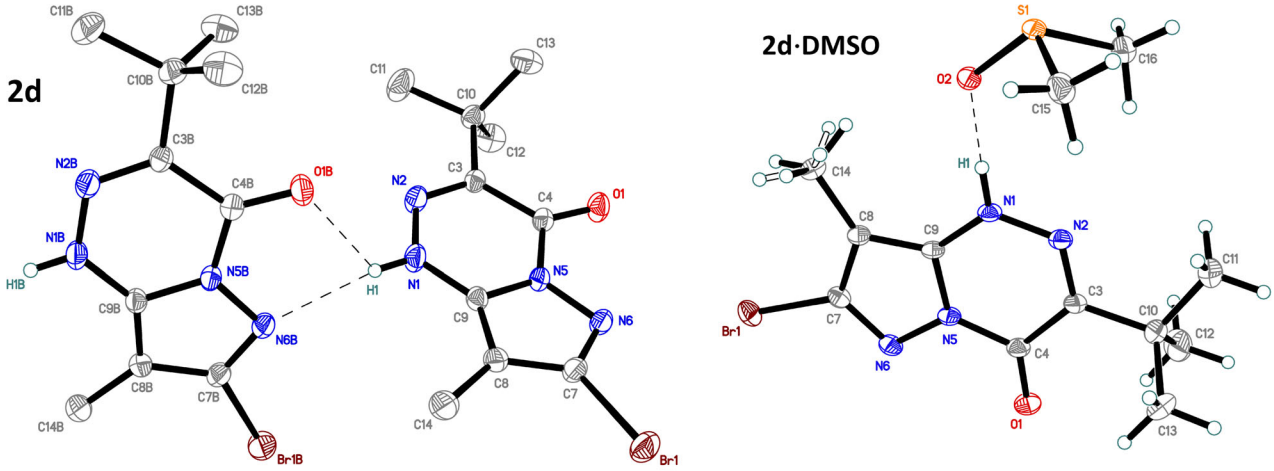
2d
C11B
C13B
C10B
C12B
C3B
N2B
C4B
O1B
N1B
H1B
N5B
C9B
N6B
C8B
C7B
C14B
Br-1B
C11
C13
C10
C12
C3
N2
C4
O1
H1
N1
C9
N5
N6
C8
C7
C14
Br-1
2d·DMSO
S1
O2
C16
C15
H1
C14
C8
C9
N1
N2
C11
C3
C10
C12
Br1
C7
N6
N5
C4
O1
C13

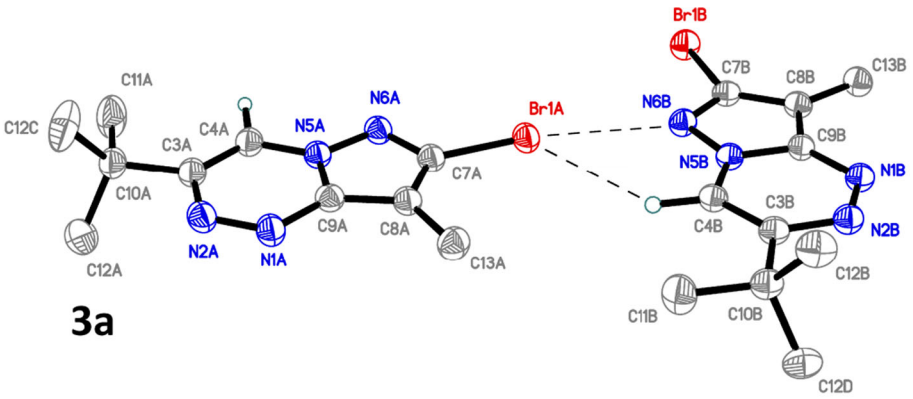
C11A
C12C
C3A
C4A
N5A
N6A
Br-1A
C7A
C10A
C9A
C8A
C13A
N2A
N1A
C12A
Br-1B
C7B
C8B
C13B
N6B
C9B
N5B
N1B
C3B
C4B
N2B
C12B
C11B
C10B
C12D
3a

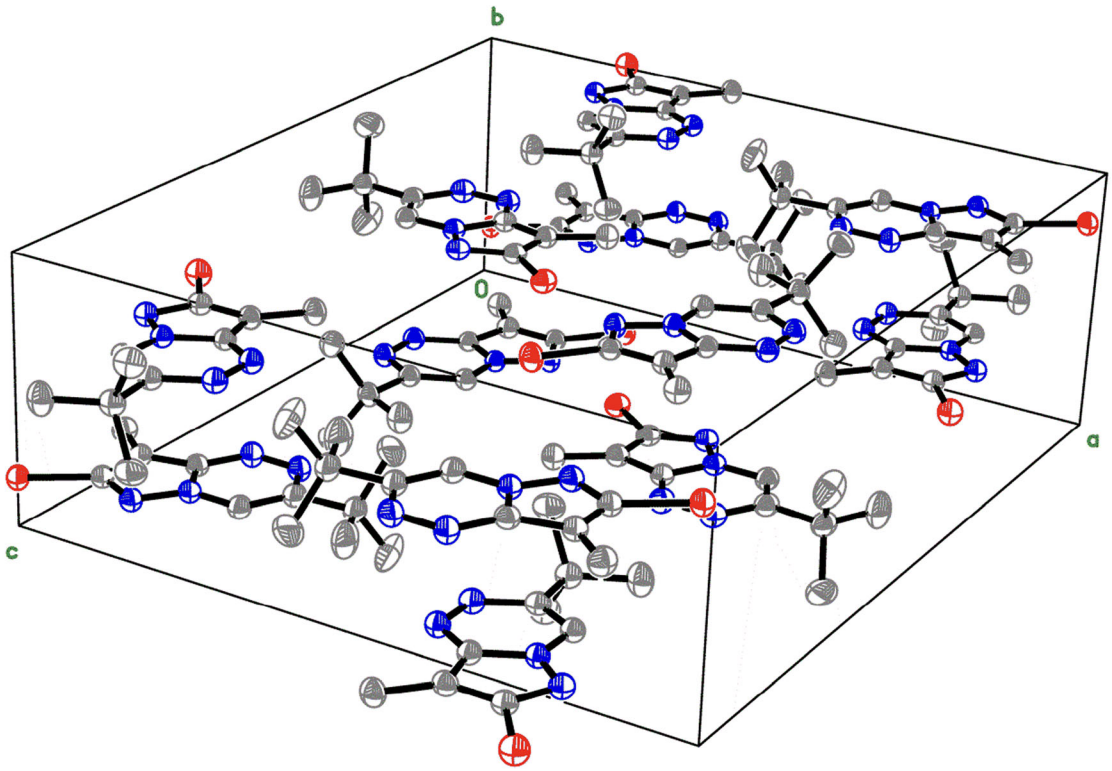
b
O
a
c

X-ray data collection and refinement

X-ray diffraction data were collected at 100 K on a Bruker Quest D8 diffractometer equipped with a Photon-III area-detector (graphite monochromator, shutterless φ- and ω-scan technique), using Mo K_α-radiation (0.71073 Å). The intensity data were integrated by the SAINT program [22] and corrected for absorption and decay using SADABS [23]. The structure was solved by direct methods using SHELXT [24] and refined on F^2 using SHELXL-2018 [25].

For **2a,b,d**, **2d•DMSO**, and **3a**: all non-hydrogen atoms were refined with individual anisotropic displacement parameters. The locations of atom H1 in **2a,b,d**, **2d•DMSO**, and all hydrogen atoms in **3a** were found from the electron density-difference map; they were refined with individual isotropic displacement parameters. All other hydrogen atoms were placed in ideal calculated positions and refined as riding atoms with relative isotropic displacement parameters. The molecule of non-solvated **2d** is disordered over 2 positions with the ratio of 0.9613(6):0.0387(6).

For **2c** and **3b,c**: all non-hydrogen atoms were refined with anisotropic displacement parameters. Positions of atoms H1A and H1B in **2c** were found from the electron density-difference map and were restrained at the distance of 0.84(3) Å from N1A/N1B, correspondingly. All other hydrogen atoms in **2c** and **3b,c** were placed in ideal calculated positions and refined as riding atoms with relative isotropic displacement parameters. A rotating group model was applied for methyl groups in **2c**. The studied crystal of **2c** was refined as a 2-component twin with the domain ratios of 0.407(2):0.593(2) and the twin law of (1.00 0.55 0.98, 0.00 -1.00 0.00, 0.01 0.00 −1.00) (the second major domain is rotated from the first one by 179.9° about reciprocal axis 1 0 0).

The SHELXTL program suite [22] was used for molecular graphics. Displacement ellipsoids are set to the 50% probability level on all figures below. See Electronic Supplementary Material (ESM) for more details on X-ray data collection and refinement.

Crystal data, data collection, and structure refinement details for **2a-d** and **3a-c** are summarized in Tables 1 and 2. Bond distances and angles, as well as additional *ORTEP* drawings, are presented in ESM for this paper. The structures have been deposited at the Cambridge Crystallographic Data Center with the reference CCDC numbers 2065233-2065240; they also contain the supplementary crystallographic data. These data can be obtained free of charge from the CCDC via http://www.ccdc.cam.ac.uk/data_request/cif.

Results and discussion

Synthesis

The starting compounds **1a,b** were prepared by cyclocondensation of 4-amino-6-*tert*-butyl-3-methylsulfanyl-1,2,4-triazin-5-one with cyanoacetic acid derivatives in pyridine (Scheme 1) [18]. Hydrolysis of the pyrazole ester moiety in **1a** and diazotization using *tert*-butyl nitrite gave 7-unsubstituted acid, which is converted to compound **2a** by halodecarboxylation [17]. Alternatively, treatment of **1a,b** with trimethylsilylbromide/*t*-BuONO followed by bromination or selective reduction of the CO_2Et group with diborane led to compounds **2b** or **2d**, respectively [18, 19]. Compound **2c** [18] was prepared by a selective C(8)-site Li/Br exchange in **2b** using *n*-butyl lithium at low temperature, and further protonation.

Aromatic triazine **3a** was synthesized from **2d** by reduction/oxidative nitration sequence [19]. In order to further investigate the structural effects of bromine substitution on the aromatic pyrazolo[5,1-*c*][1,2,4]triazine system, we set the task of switching the oxygen atom to hydrogen at the C4 position and comparing the structure of the obtained compounds. Novel 4-unsubstituted pyrazolotriazines **3b**,**c** were prepared by decarboxylative N(1)-acylation of the carboxylic acid **1b** with

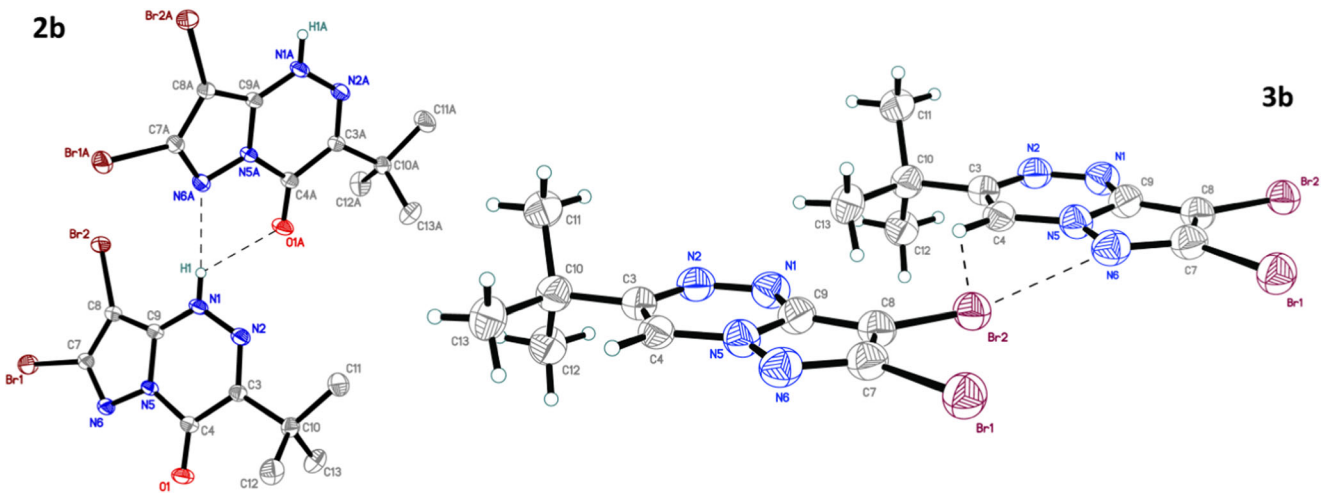

Fig. 3 Molecular structures of **2b** and **3b**. H-atoms of methyl groups for **2b** are omitted; displacement ellipsoids are shown at the 50% probability level

di-*tert*-butyl dicarbonate [20] and diazotization/bromination sequence. Reduction of N(1)-Boc protected dibromopyrazolotriazine **4** with further dehydrative aromatization of hydroxytriazine **5** in acidic media gave a mixture of compounds **3b** and **3c** in 57% overall yield. Formation of compound **3c** can be explained in terms of electrophilic heteroaromatic *ipso*-substitution [26] of Br^+ by H^+. Crystals were successfully grown for all the isolated compounds and X-ray diffraction analyses were carried out.

Crystal structure discussion

Molecular structure description

Series of 7- or 8-monobromo compounds **2a**,**c** and **3a,c** are crystallized from ethyl acetate/dimethylsulfoxide (10:1) mixture in the monoclinic (the $P2_1/c$ space group for **2a** and $P2_1/n$ for **3c**), triclinic (the $P\bar{1}$ space group for **2c**), and orthorhombic (*Pnma* for **3a**) crystal systems without inclusion of solvent molecules into the crystal lattice. Compound **2d** was simultaneously crystalized from ethyl acetate/DMSO (10:1) mixture at r.t. in two forms: as single crystals of non-solvated 7-bromo-3-*tert*-butyl-8-methylpyrazolo[5,1-*c*][1,2,4]triazin-4(1*H*)-one **2d** in the orthorhombic crystal system (the *Pbca* space group), and as a 1:1 solvate with dimethylsulfoxide **2d·DMSO** in the triclinic crystal system (the $P\bar{1}$ space group). 7,8-Dibromo pyrazolotriazines **2b** and **3b** were also crystallized from EtOAc/DMSO (10:1) mixture in the orthorhombic (*Pbca*) and monoclinic groups ($P2_1/n$) respectively. All studied crystal structures (Figs. 1, 2, and 3) exhibit similar geometries; yet, some subtle differences will be mentioned. Results of X-ray diffraction studies for compounds **2a-d** and **3a-c** are presented in Tables 3, 4, 5, and 6.

Table 3 Selected bond distances in **2a, 2c** and **3c** (Å)

Bond	2a	2c	3c
Br–C8	1.8658(13)	-	-
Br–C7	-	1.854(5)	1.8619(11)
O–C4	1.2132(16)	1.209(6)	-
N1–N2	1.3425(17)	1.340(6)	1.3153(13)
N1–C9	1.3478(18)	1.351(6)	1.3460(14)
N2–C3	1.3081(18)	1.295(6)	1.3668(13)
N5–C9	1.3670(17)	1.378(6)	1.3938(13)
N5–N6	1.3686(16)	1.365(6)	1.3492(13)
N5–C4	1.4011(18)	1.387(7)	1.3504(14)
N6–C7	1.3349(19)	1.331(7)	1.3523(14)
C3–C4	1.478(2)	1.492(7)	1.3788(15)
C7–C8	1.4035(19)	1.410(7)	1.3880(15)
C8–C9	1.380(2)	1.390(7)	1.3941(15)

Table 4 Selected bond distances in **2d, 2d·DMSO** and **3a** (Å)

Bond	2d	2d·DMSO	3a
Br–C7	1.8652(18)	1.8670(8)	1.8629(19)
O–C4	1.216(2)	1.2208(10)	-
C8–C14	1.495(3)	1.4953(11)	1.489(3)
N1–N2	1.339(2)	1.3335(10)	1.308(2)
N1–C9	1.350(2)	1.3521(10)	1.354(2)
N2–C3	1.305(2)	1.3076(10)	1.381(3)
N5–N6	1.371(2)	1.3620(10)	1.345(2)
N5–C9	1.371(2)	1.3751(9)	1.384(2)
N5–C4	1.393(2)	1.3928(11)	1.360(2)
N6–C7	1.328(2)	1.3284(11)	1.350(2)
C3–C4	1.471(2)	1.4694(11)	1.366(3)
C7–C8	1.405(2)	1.4070(11)	1.388(3)
C8–C9	1.385(3)	1.3828(11)	1.398(3)

A slight increase in the C7–Br bond length compared to C8–Br for compounds **2c** (1.854 (5) Å) and **2a** (1.8658 (13) Å), respectively, is observed, which demonstrated the different π-electron density distribution in the conjugated system. The other bond distances are similar in both molecules. We were able to successfully switch the oxygen atom in 4-oxo derivative **2c** to hydrogen and structurally characterize novel 7-bromo-3-*tert*-butylpyrazolo[5,1-*c*][1,2,4]triazine **3c** as well. The latter compound was investigated by X-ray diffraction method, and it was found that, for **3c**, the N1–N2, C3–C4, and N5–N6 bond lengths are shorter than the corresponding bonds in compounds **2a**,**c** (Table 3), which indicate substantial increase in triazine ring conjugation for **3c** compared to **2a** and **2c**. The Br atom in aromatic derivative **3c** deviates more from the plane than in compounds **2a**,**c** (~4° for **3c** and ~2° for **2a**,**c**), which can be explained by non-valence interactions, e.g., Br···N2 = 3.35 Å, H4···N1 = 2.35 Å (Table 6). The C–C bond lengths within the

Table 5 Selected bond distances in **2b** and **3b** (Å)

Bond	2b	3b
Br–C7	1.8569(17)	1.851(7)
Br–C8	1.8576(16)	1.855(6)
O–C4	1.213(2)	-
N1–N2	1.341(2)	1.307(8)
N1–C9	1.345(2)	1.349(9)
N2–C3	1.311(2)	1.373(9)
N5–C9	1.365(2)	1.382(9)
N5–N6	1.368(2)	1.354(8)
N5–C4	1.402(2)	1.368(8)
N6–C7	1.327(2)	1.344(9)
C3–C4	1.471(2)	1.384(9)
C7–C8	1.407(2)	1.398(9)
C8–C9	1.380(2)	1.387(9)

Table 6 Intramolecular hydrogen-bond parameters (Å, °) in **2a-d**, and **3c**

Compound	*D*—H···*A*	*D*—H (Å)	H···*A* (Å)	*D*···*A* (Å)	*D*—H···*A* (°)
2a	N1—H1···N6^{i}	0.86(2)	2.02(2)	2.8647(16)	170(2)
2b	N1—H1···O1^{ii}	0.81(3)	2.57(3)	3.029(2)	118(2)
	N1—H1···N6^{ii}	0.81(3)	2.17(3)	2.967(2)	170(3)
2c	N1—H1···O1^{iii}	0.81(3)	2.59(6)	3.266(6)	142(7)
	N1—H1···N6^{iii}	0.81(3)	2.23(5)	2.944(6)	148(8)
2d	N1—H1···O1^{iii}	0.84(3)	2.41(3)	2.969(2)	125(3)
	N1—H1···N6^{iii}	0.84(3)	2.21(3)	3.015(2)	160(3)
2d·DMSO	N1—H1···O1	0.910(16)	1.753(16)	2.6624(9)	177.4(15)
3c	C(4)—H(4)···N(1)^{iv}	0.95	2.35	3.2935(13)	172

Symmetry codes: (i) *x*, −*y*+3/2, *z*+1/2; (ii) −*x*+3/2, *y*−1/2, *z*; (iii) −*x*+3/2, *y*+1/2, *z*; (iv) *x*−1, *y*, *z*

^{t}Bu group and distance C3–C10(Me_3) vary from 1.522(2) Å to 1.549(9) Å for all compounds.

It is worth noting that the crystallization of **2d** carried out under the same conditions gave two types of crystals—non-solvated and with inclusion of DMSO molecules into the crystal lattice. Both compounds have a similar structure, but the bromine atom in non-solvated **2d** deviates more from the pyrazole plane (~2° for **2d** and <1° for **2d·DMSO**), which can be explained by the large contribution of non-valent intermolecular interactions. The added methyl group at the C8 position and switching the oxygen atom to hydrogen at the C4 site was expected to change the molecular geometry—the Br–C7–C8–C9 torsion angle for **3a** is 180.000(1)° compared to **3c** (175.93(8)°). It is interesting to note that this angle remains practically unchanged for 4-oxopyrazolotriazines **2d** (178.20(14)°) and **2c** (178.2(4)°). Other torsion angles in compound **3a** were approximately equal to 180°, which indicated a more pronounced aromatic character. The distances C8–C14 and C7–Br are similar for all compounds and vary from 1.489(3) Å to 1.4953(11) Å and from 1.8629(19) Å to 1.8670(8) Å, respectively.

Finally, the crystal structures of 7,8-dibromo-4-oxopyrazolo[5,1-*c*][1,2,4]triazine **2b** and its 4-unsubstituted analog **3b** were investigated. Both compounds readily produced single crystals and their structures were determined by X-ray diffraction. The C7–Br and C8–Br bond lengths in 7,8-dibromopyrazolo[5,1-*c*][1,2,4]triazines **2b** and **3b** have similar values which vary from 1.851(7) Å (C7–Br for **3b**) to 1.8576(16) Å (C8–Br for **2b**). The two bromine atoms in **2b** deviate from the plane by ~2°, while the corresponding atoms in **3b** are held practically coplanar towards the whole bicyclic system. Similarly, the C10(Me_3) moiety in 4-oxopyrazolotriazine **2b** is located outside of the triazine ring (with a deviation of about 4°), while the corresponding atom in 4-unsubstituted analog **3b** is located practically within the plane (N1–N2–C3–C10 = 179.9(6)°). The N1–N2, C3–C4, and N5–C4 bond lengths are significantly shorter in **3b** when compared to **2b**, which proved the presence of a conjugated aromatic system in **3b**.

Non-valence interactions

The molecules form infinite 1D chains *via* hydrogen bonding along the *c* (**2a**) or *b* (**2b**, **2c**, **2d**, **2d·DMSO, 3c**) axes: atom H1 interacts with both N6 and O1 atoms of a neighboring molecule (Figs. 1, 2, and 3). The experimental N1–H1 bond distances in all the studied compounds vary from 0.81(3) Å to 0.95Å (Table 6). It should be mentioned that these interactions are somewhat different among the studied crystals. Thus, the shortest donor···acceptor (*D*···*A*) distance and the largest *D*—H···*A* angle correspond to the bond N1—H1···O1 in **2d·DMSO**, while the longest H-bond among the series was observed for compound **3c**. On the contrary, C8–Me and C8–Br substituted analogs **3a,b** do not tend to form any significant H-bonds. All the 4-oxo derivatives except for **2a** (Fig. 1) exhibit two types of hydrogen bonds between N1H and N6 or O1 atoms. It is worth noting that both hydrogen bonds are nearly equal in **2b** and **2d** (Figs. 2 and 3 and Table 6).

C8–Br in compound **2a** is coordinated with N5 and N2 atoms of the nearby molecules at nearly identical distances of 3.35–3.38Å. Similarly, C7–Br in compounds **2b**,**d** is coordinated with N2 (N2···Br = 3.41–3.42Å). However, bromine in a crystal lattice of analogous compound **2c** with a vacant C8 position is surrounded by *t*-Bu groups and did not form any significant halogen bonds [27], apparently due to the competing H-bonding.

Molecules of compound **3c** exhibited short contacts (N2···Br = 3.347(1)Å) which resemble that for **2b** and **2d**. An addition of C8–Me substituent to the aromatic pyrazolotriazine **3c** led to considerable changes in the intermolecular interactions. Thus, every second molecule of **3a** provided the bromine to form a pronounced halogen bond with the nearby azo-heterocycle (N6···Br = 3.014Å, Fig. 2). In compound **3b**,

C8–Br and N6 atoms also form halogen bonds with the distance of 3.254(7) Å (Fig. 3).

Conclusions

To summarize, a total of eight isomeric pyrazole ring brominated 3-*tert*-butylpyrazolo[5,1-*c*][1,2,4]triazines have been for the first time investigated by X-ray single crystal diffraction analyses. Novel 7-bromo- and 7,8-dibromo-3-*tert*-butylpyrazolo[5,1-*c*][1,2,4]triazines were synthesized by reduction of triazine carbonyl with dehydrative aromatization in acidic media, and their XRD structural features were compared with that of the 4-oxo analogs. The experimental results revealed a marked increase in the aromatic character on switching oxygen atom in C4 position to hydrogen, which is indicated by the shortening of the heterocyclic bond lengths and smoothing of the torsion angles. Non-valence interactions and different packing modes depending upon the position of the bromine atoms were also considered.

Supplementary Information The online version contains supplementary material available at https://doi.org/10.1007/s11224-021-01768-0.

Acknowledgements Crystal structure determination was performed in the Department of Structural Studies of Zelinsky Institute of Organic Chemistry, Moscow.

Author contribution The authors of the current manuscript Sergey M. Ivanov and Denis S. Koltun contributed equally to this work. All authors read and approved the final manuscript.

Data Availability The structures have been deposited at the Cambridge Crystallographic Data Center with the reference CCDC numbers 2065233-2065240; they also contain the supplementary crystallographic data. These data can be obtained free of charge from the CCDC via http://www.ccdc.cam.ac.uk/

The online version of this article contains electronic supplementary material (ESM) on crystal structures, IR, NMR, and HRMS data for all new compounds.

Code availability Not applicable.

Declarations

Conflict of interest The authors declare no competing interests.

References

1. Nifant'ev IE, Vinogradov AA, Minyaev ME, Komarov PD, Lyssenko KA, Birin KP, Dyadchenko VP, Ivchenko PV (2019) The structural diversity of heterocycle-fused potassium cyclopentadienides. RSC Adv 9:29195–29204. https://doi.org/10.1039/C9RA04587B
2. Lewis AK, Caddick S, Geoffrey F, Cloke N, Billingham NC, Hitchcock PB, Leonard J (2003) Synthetic, structural, and mechanistic studies on the oxidative addition of aromatic chlorides to a palladium (N-heterocyclic carbene) complex: relevance to catalytic amination. J Am Chem Soc 125(33):10066–10073. https://doi.org/10.1021/ja035565k
3. Lotesta SD, Kiren S, Sauers RR, Williams LJ (2007) Spirodiepoxides: heterocycle synthesis and mechanistic insight. Angew Chem Int Ed 46:7108–7111. https://doi.org/10.1002/anie.200701401
4. Vitaku E, Smith DT, Njardarson JT (2014) Analysis of the structural diversity, substitution patterns, and frequency of nitrogen heterocycles among U.S. FDA Approved Pharmaceuticals. J Med Chem 57(24):10257–10274. https://doi.org/10.1021/jm501100b
5. Kerru N, Gummidi L, Maddila S, Gangu KK, Jonnalagadda SB (2020) A review on recent advances in nitrogen-containing molecules and their biological applications. Molecules 25(8):1909. https://doi.org/10.3390/molecules25081909
6. Reid RC, Yau M-K, Singh R, Lim J, Fairlie DP (2014) Stereoelectronic effects dictate molecular conformation and biological function of heterocyclic amides. J Am Chem Soc 136(34):11914–11917. https://doi.org/10.1021/ja506518t
7. Gaweda K, Plazinska A, Plazinski W (2020) Conformations of saturated five-membered heterocycles evaluated by mp_2 calculations. Chem Heterocycl Compd 56(12):1599–1604
8. Kleinpeter E (2004) Conformational analysis of saturated heterocyclic six-membered rings. Adv Heterocycl Chem 86:41–127. https://doi.org/10.1002/chin.200428300
9. Ponnuswamy MN, Gromiha MM, Malathy Sony SM, Saraboji K (2006) Conformational aspects and interaction studies of heterocyclic drugs. Top Heterocycl Chem 3:81–147. https://doi.org/10.1007/7081_027
10. Charushin V, Rusinov V, Chupakhin O (2008) 1,2,4-Triazines and their benzo derivatives. Compr Heterocycl Chem III 9:95–196. https://doi.org/10.1016/B978-008044992-0.00802-6
11. Sonawane RP, Sikervar V, Sasmal S (2020) 1,3,5-Triazines. Elsevier reference collection in Chemistry, Molecular Sciences and Chemical Engineering in press. https://doi.org/10.1016/B978-0-12-818655-8.00018-4
12. Voinkov EK, Drokin RA, Ulomskii EN, Chupakhin ON, Charushin VN, Rusinov VL (2020) Methods of synthesis for the azolo[1,2,4]triazines. Chem Heterocycl Compd 56(10):1254–1273. https://doi.org/10.1007/s10593-020-02808-z
13. Rusinov VL, Ulomskii EN, Chupakhin ON, Charushin VN (2008) Azolo[5,1-*c*][1,2,4] triazines as a new class of antiviral compounds. Russ Chem Bull Int Ed 57(5):985–1014. https://doi.org/10.1007/s11172-008-0130-8
14. von Keutz T, Williams JD, Kappe CO (2020) Continuous flow C-glycosylation via metal–halogen exchange: process understanding and improvements toward efficient manufacturing of remdesivir. Org Process Res Dev 24(10):2362–2368. https://doi.org/10.1021/acs.oprd.0c00370
15. Knapp RR, Tona V, Okada T, Sarpong R, Garg NK (2020) Cyanoamidine cyclization approach to remdesivir's nucleobase. Org Lett 22(21):8430–8435. https://doi.org/10.1021/acs.orglett.0c03052
16. Ivanov SM, Traven VF, Minyaev ME (2020) Structural studies of 3-*tert*-butyl-8-(methylchalcogenyl)pyrazolo[5,1-*c*][1,2,4]triazin-4(1H)-ones. Struct Chem 31:1457–1470. https://doi.org/10.1007/s11224-020-01533-9
17. Ivanov SM, Mironovich LM, Kolotyrkina NG, Shestopalov AM (2019) Synthesis and chemical properties of 8-lithio-4-oxopyrazolo[5,1-*c*][1,2,4]triazines. Russ Chem Bull Int Ed 68:614–622. https://doi.org/10.1007/s11172-019-2464-9
18. Ivanov SM, Shestopalov AM (2019) Metalated Azolo[1,2,4]triazines. I. Synthesis of 2-(6-tert-butyl-5-oxo-4,5-dihydro-1,2,4-triazin-3(2h)-ylidene) acetonitriles via ring opening degradation of 3-*tert*-Butyl-7-lithio-4-oxo-4H-pyrazolo[5,1-*c*][1,2,4]triazin-1-ides. J Heterocyclic Chem 56:2210–2220. https://doi.org/10.1002/jhet.3615

19. Ivanov SM, Dmitrienko AO, Medvedev MG, Mironovich LM (2019) Metalated azolo[1,2,4]triazines. II. Generation, C(4)-substituent dependent stability and electrophile trapping of 7-lithiopyrazolo[5,1-*c*][1,2,4]triazines. J Organomet Chem 896:168–182. https://doi.org/10.1016/j.jorganchem.2019.06.009
20. Ivanov SM, Lyssenko KA, Mironovich LM, Shestopalov AM (2019) Decarboxylation and electrophilic substitution in 3-*tert*-butyl-4-oxopyrazolo[5,1-*c*][1,2,4]triazines. Russ Chem Bull Int Ed 68:1714–1722. https://doi.org/10.1007/s11172-019-2615-z
21. Ivanov SM, Mironovich LM, Kolotyrkina NG, Minyaev ME (2021) Synthesis of (3-*tert*-Butylpyrazolo[5,1-*c*][1,2,4]triazin-4-yl)phosphine Oxides. Russ J Org Chem 57:47–57. https://doi.org/10.1134/S1070428021010073
22. Bruker (2018) APEX-III. Bruker AXS Inc., Madison, Wisconsin, USA
23. Krause L, Herbst-Irmer R, Sheldrick GM, Stalke D (2015) Comparison of silver and molybdenum microfocus X-ray sources for single-crystal structure determination. J Appl Crystallogr 48:3–10. https://doi.org/10.1107/S1600576714022985
24. Sheldrick GM (2015) SHELXT - Integrated space-group and crystal-structure determination. Acta Cryst A71:3–8. https://doi.org/10.1107/S2053273314026370
25. Sheldrick GM (2015) Crystal structure refinement with SHELXL. Acta Cryst C71:3–8. https://doi.org/10.1107/S2053229614024218
26. Bonesi SM, Fagnoni M (2010) The aromatic carbon–carbon ipso-substitution reaction. Chem Eur J 16:13572–13589. https://doi.org/10.1002/chem.201001478
27. Cavallo G, Metrangolo P, Milani R, Pilati T, Priimagi A, Resnati G, Terraneo G (2016) The halogen bond. Chem Rev 116:2478–2601. https://doi.org/10.1021/acs.chemrev.5b00484